JOINT INFLUENCE OF RESISTIVITY ANISOTROPY AND INHOMOGENEITY FOR A SINGLE DIPPING INTERFACE BETWEEN ISOTROPIC OVERBURDEN AND ANISOTROPIC BASEMENT

Dr. Evgueni Pervago, IMP, Mexico City, Mexico
Dr. Aleksandr Mousatov, IMP, Mexico City, Mexico
Dr. Vladimir Shevnin, IMP, Mexico City, Mexico

Abstract

The media with joint influence of anisotropy and inhomogeneity have large practical interest. The difficulty of practical anisotropy studying with collinear arrays results from the fact, that anisotropy exhibits itself weaker, than inhomogeneity at equal resistivity contrasts. The relative anisotropy and inhomogeneity influence is considered with the help of mathematical modeling for gentle dipping interface with anisotropic basement. The algorithm is based on the integral equations' method for 3D models with anisotropy.

This model is considered for three different directions of strike of dipping interface and strike of anisotropic basement, in comparison with isotropic model of dipping interface and horizontally - layered model with the anisotropic basement. The modeling data are submitted as azimuthal diagrams and results of their spectral analysis. Spectral analysis helps to receive some diagnostic parameters for anisotropic - inhomogeneous media.

All resistivity arrays on sensitivity to anisotropy are divided into two groups: collinear arrays (Schlumberger, pole-pole, pole-dipole, dipole axial) with the axes ratio equal λ, and non-collinear arrays (dipole equatorial, T-array, etc.) with sensitivity up to λ^5. Most sensitive to inclined contact is dipole axial array, and it is the least sensitive to anisotropy.

The inhomogeneity influence is displayed in the first harmonic of azimuthal diagrams's spectrum, and anisotropy - in the second harmonic. The inhomogeneity also influences on the second harmonic. The absence of the first harmonic (and following odd ones) testifies to absence of inhomogeneity influence. For comparison of relative influence of anisotropy and inhomogeneity, it is necessary to consider the ratio of the sum odd to the sum of even harmonics. When O/E ratio is >1, the inhomogeneity influence prevails, and when <1 - the anisotropy influence prevails. At joint influence of basement anisotropy ($\lambda = 2$) and dipping interface (dip is 5°), the anisotropy influence prevails only for non-collinear arrays.

Introduction

The study of media, in which inhomogeneity and anisotropy or layering and anisotropy influence jointly, represents rather complex and not fully investigated problem. The traditional azimuthal survey technique, using collinear arrays Schlumberger or Wenner for the study of azimuthal media meets great difficulties. As a rule the influence of anisotropy for such arrays is displayed weaker than that of inhomogeneities.

If the model for sounding or profiling is made of two blocks with a resistivity contrast equal to 10, then apparent resistivities' difference also can reach 10. Anisotropic model, consisting of two interstratified thin rock layers of equal thickness and with the same resistivity contrast (10), gives a true anisotropy coefficient λ. Using this model, the difference in apparent resistivities for any collinear arrays is only equal to 1.7. That means, that with the joint influence of anisotropy and inhomogeneities

1

(generated by the same resistivity contrast) the influence of anisotropy will be 6 times weaker then that of the inhomogeneities. In case of nonlinear arrays (for example, dipole equatorial) for a medium with a true anisotropy coefficient $\lambda=1.7$, we record the Dipole Equatorial Array (DEA) azimuthal diagram's axes ratio equal to $\lambda^5=14$!

Professor A.S.Semenov first published a theoretical estimation of this high sensitivity to anisotropy by the dipole equatorial array in (1975). In this case (at identical resistivities' contrasts, as in an above example) the anisotropy influence exceeds the effect of the inhomogeneity.

In the majority of practical cases when collinear arrays are used, either anisotropy is shown together with inhomogeneities and is almost invisible on their background, or anisotropy is absent and influence of inhomogeneities, deforming the polar diagrams, is wrongly accepted for anisotropy. In Watson and Barker article (1999) and Watson theses (1999) many typical cases of such pseudo-anisotropy or joint appearance of anisotropy and inhomogeneities are considered. The situation becomes further complicated by the influence of small near-surface inhomogeneities near to the current and potential electrodes (geological noise). The level of geological noise (in average field condition) can reach 8-12% (Electrical prospecting..., 1994). Therefore it is very important to choose a system of survey, which maximizes anisotropy influence in comparison with that of inhomogeneities.

There is also one more serious problem. When Schlumberger or Wenner arrays are rotated around their center point, the influence of anisotropy is indistinguishable from that of inhomogeneity. Inhomogeneity can also produce ellipse-like diagrams. To avoid this mistake it is necessary to apply non-symmetrical rotation or non-symmetrical array (or both). The Offset-Wenner array (Watson and Barker, 1999) gave new possibility for discrimination between influence of anisotropy and inhomogeneity. In fact this is the traditional Wenner array but with a non-symmetrical rotation only. Unfortunately Wenner array, as any other collinear array, has very low sensitivity to anisotropy, which easily can be overcome by inhomogeneity.

In Bolshakov et al. (1997, 1998) publications, great attention is given to questions of joint show of an anisotropy and inhomogeneity. The spectral approach, allowing estimates of the main factors, influencing the azimuthal diagram, is offered. The model of a single dipping interface between isotropic overburden and anisotropic basement, considered in given work, seems to us a good basis for continuation of such study, as it simultaneously includes elements of layered medium, inhomogeneity and anisotropy. Such model gives weaker influence of an inhomogeneity in comparison with the earlier investigated model of vertical contact. At small dip angle it is possible to receive influence of an inhomogeneity without any of the array's electrodes crossing the dipping interface by array's electrodes, which gives additional distortions of azimuthal diagrams.

Tasks of the present work are:

1. Studying joint influence of anisotropy and inhomogeneities, anisotropy and layering.

2. Comparing advantages and disadvantages of various types of arrays.

The algorithm used in the given work, is based on integral equations' method. This program was developed for account of 3D well logging problems with anisotropy, and was used for accounting problems on the earth surface. The basic accounted model has the isotropic overburden thickness (at the center of rotation) - 1 м, sounding spacings from 0.1 up to 10 m with a step 10 points for decade, anisotropy coefficient of the bottom layer - 2, and the resistivities difference between the first and second layer - 10. The model with $\rho_2 < \rho_1$ is named in the text R1, and the model with $\rho_2 > \rho_1$ is named R2. The dip angle is equal to 5°. This angle was selected because at the maximal spacing 8 - 10 m and the first layer thickness 1 m, the array does not get in area of an interface outcrop. Several variants of this model are considered: when the strike of dipping interface is parallel to the strike of anisotropy plane (fig.1, 4), when these two strikes are perpendicular (fig.1, 3), when these differ on 45° and when the anisotropy is absent (fig.1, 2). In selection these models we followed to Watson (1999). For

comparison the model of horizontally - layered medium with the anisotropic basement is also submitted (fig.1, 1).
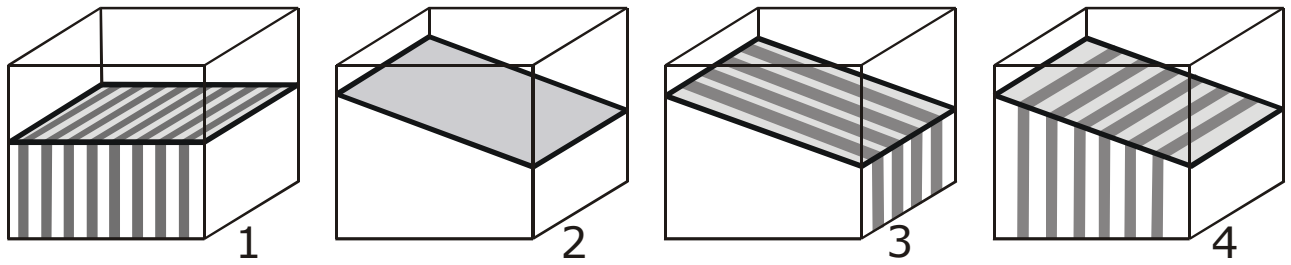

Fig.1. Four based models used for azimuthal diagrams' calculation: 1- two-layered model with anisotropic basement; 2 – dipping interface; 3 – anisotropy in basement, oriented across dipping interface's strike; 4 - anisotropy in basement, oriented along dipping interface's strike.

Modeling Results

The account of azimuthal apparent resistivity is carried out depending on array spacing, array azimuth and for several different (collinear and non-linear) arrays: dipole equatorial, dipole axial and some others.

The account results can be submitted as azimuthal diagrams (fig.2) and sounding curves for separate azimuths (fig.3). On small spacings, the azimuthal diagrams look like circles, since reflect only the isotropic overburden. With spacings growth, the ARS diagrams for DEA became extended along strike of anisotropic formation in accordance with anisotropy paradox. We consider as DEA azimuth the direction between centers of AB and MN dipoles (in contrast to Habberjam). ARS diagrams' radii
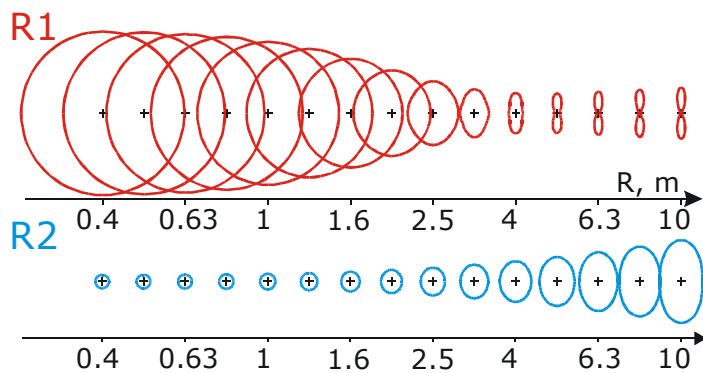

Fig.2. An example of the azimuthal diagrams varied with spacing for two-layered model (fig.1) and dipole equatorial array.
R1 – $\rho_2 < \rho_1$; R2 - $\rho_2 > \rho_1$.

for $\rho_2<\rho_1$ decrease, since the resistivity of the bottom layer is lower than top or grow for a case $\rho_2>\rho_1$. For a case $\rho_2>\rho_1$ eccentricity of the diagrams it is essentially smaller, than for $\rho_2<\rho_1$ (fig.2). There is no break in anisotropy paradox for dipole equatorial array above two-layer model in contrast to collinear arrays (Electrical prospecting..., 1994).

VES curves on fig.3 are submitted for two-layer models with $\rho_2<\rho_1$ and $\rho_2>\rho_1$, both for isotropic and anisotropic basement. In the latter case account is
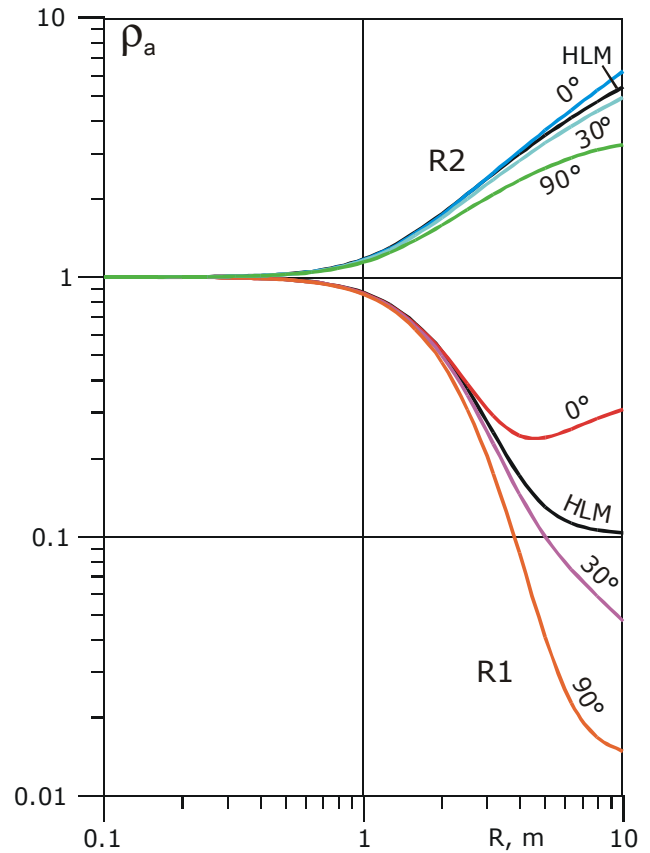

Fig.3. VES Curves for isotropic (HLM) and anisotropic layered models for different azimuths of DE array.

executed for DE array, for which the difference of curves for different azimuths is maximal. On fig.3 it is visible, that approaching to the right asymptote for a case $\rho_2 < \rho_1$ occurs faster, than for $\rho_2 > \rho_1$ (this fact is well known). But also the curves' difference for different azimuths in the first case also grows faster, i.e. the case with resistive basement is less favorable for its anisotropy study.

The first R1 model (fig.1, 4) has orientation of anisotropy plane along strike of dipping interface. The results for different arrays are submitted on fig.4-8. The analysis of azimuthal diagrams' spectra is executed and the graphs of the 1-st and 2-nd harmonics as spacing function (fig.4-5) are displayed. In a case of horizontally layered medium, the first harmonic of spectrum is absent. It appears only under influence of horizontal inhomogeneities (Bolshakov et al., 1997). The similarity of the first harmonics for T and DA arrays, for model with anisotropic (TA, DAA) and isotropic (IC_T, IC_DAA) basement (the graphs on fig.4 are constructed in linear scale along Y axis) proves this idea. The graphs of the first harmonics of spectrum (fig.4) on small spacings begin from zero, then achieve maximum and at large spacings again leave to zero. The greatest amplitude of the first harmonic has dipole axial array (DAA), which is the most sensitive to interface inclination. Dipole equatorial (DEA) and T - array give the similar graphs, but their maxima are on smaller spacings, than for dipole axial array, because of greater depth of investigation in comparison with DAA. The large similarity of the first harmonics' graphs for three models with fig.1 – dipping interface without anisotropy (IC) and with anisotropy, which strike is parallel to strike of contact and parallel to its dip emphasizes that fact, that the first harmonic reflects only influence of dipping interface and it practically is not influenced by presence and strike of anisotropy. This fact allows approaching to decompose of anisotropy and inhomogeneity influence with the help of ARS diagrams' spectral analysis. Particularly the first harmonic of spectrum reflects an inhomogeneities' influence.
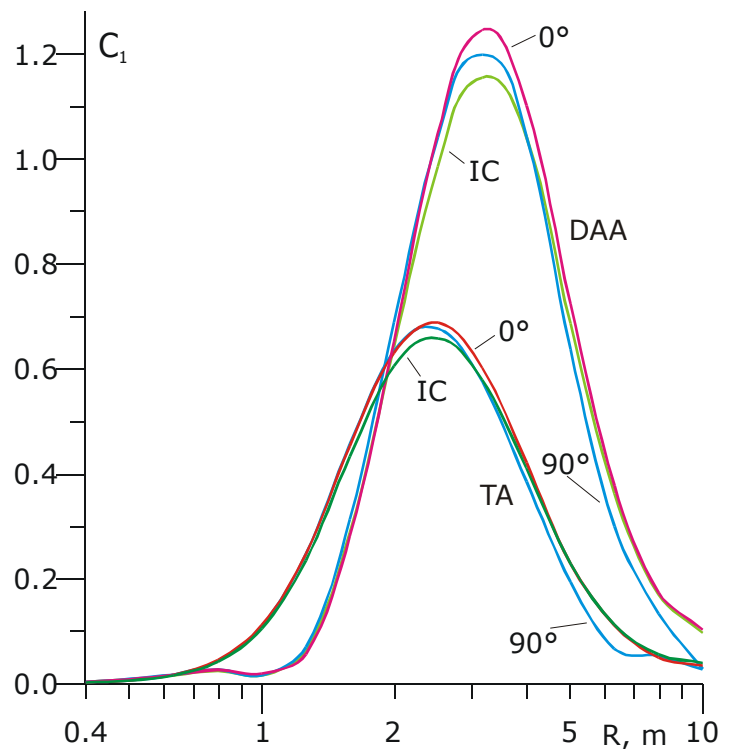

Fig.4. The first harmonics of azimuthal diagram's spectra for different models: dipping interface without anisotropy and models 3 - 4 from fig.1 (for spacing 3.1 m).
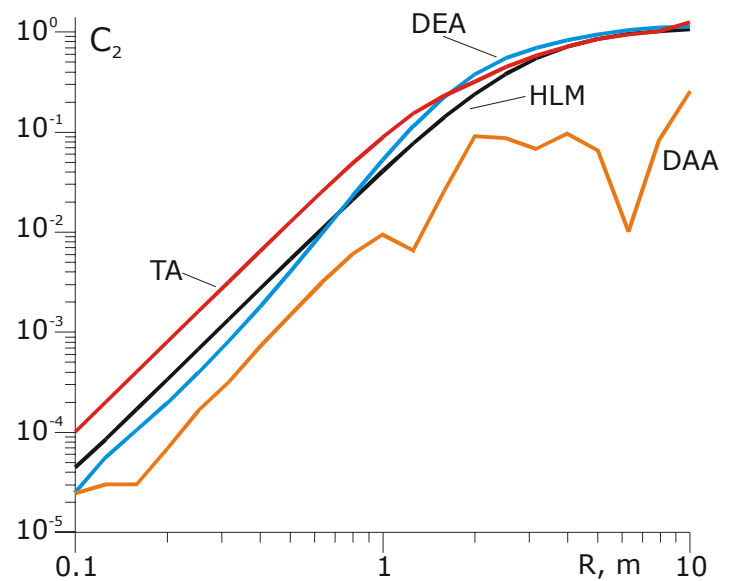

Fig.5. The graphs of the second harmonic of spectrum for several arrays for model 4 (fig.1).

The graphs of the second harmonics (fig.5) (graphs are constructed in logarithmic scale along Y axis) are similar for different arrays and reflect growth of arrays' sensitivity to an anisotropy of the bottom layer with the spacing growth. The second harmonics' graphs are similar for T and dipole

equatorial array, while DA array (curve 4) appreciably concedes on sensitivity to anisotropy, on the great spacings approximately on the order. The second harmonic's graph for horizontally - layered model (1) does not differ greatly from the diagram for model with dipping interface and anisotropic basement (2, 3). Their similarity shows the primary influence of anisotropy on the second harmonic of spectrum. But the inhomogeneity has also minor influence on the second harmonic.

The zero harmonic of spectrum allows seeing influence of horizontal layering of the model. Quantitative interpretation of zero harmonics' graphs as VES curves (Bolshakov et al., 1997) gives boundary depth estimation under sounding site with an error from 0.4 up to 4 % for different arrays. The resistivity of the top isotropic layer thus is determined practically precisely; the resistivity of the second (anisotropic) layer is underestimated on ρ_m value on 25-30%.

Fig.6 is essentially important for understanding of anisotropy and inhomogeneity ratio, on which the amplitude graphs of the first and second harmonics for T and DAA arrays are displayed together with the graphs of apparent anisotropy coefficient (all graphs are constructed in logarithmic scale along Y axis). On λ_a graphs, the anisotropy influence begins to grow for T array after $r/h = 1.5$, and for dipole axial array after $r/h = 4$. λ_a graphs on small spacings begin with one (for the top isotropic layer) and then the graphs grow achieving 1.8 for DA array and 20 for TA. At the moment of λ_a growth beginning on the graphs of harmonics the reduction of differences in amplitudes of the first and second harmonics appears and then fast growth of influence of the second one begins. For T-array there is spacing interval (after 3 m), when the second harmonic exceeds the first one (anisotropy influence exceeds inhomogeneity influence), and for dipole axial array such situation does not come at all. It means, that the inhomogeneity influence (or pseudo-anisotropy) for collinear arrays in similar model always is higher than influence of true anisotropy. Only non-collinear arrays can give anisotropy
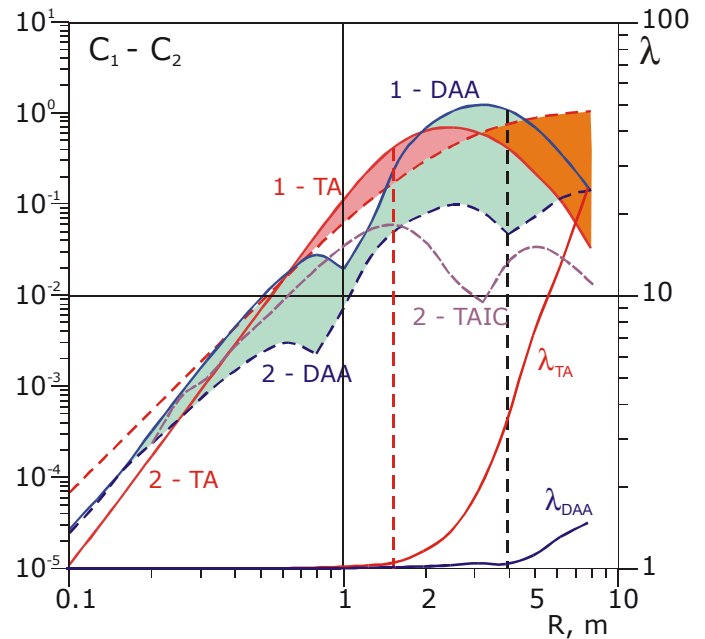

Fig.6. Comparison of the first and second harmonics for dipole axial and T-arrays and graphs of apparent anisotropy coefficient.
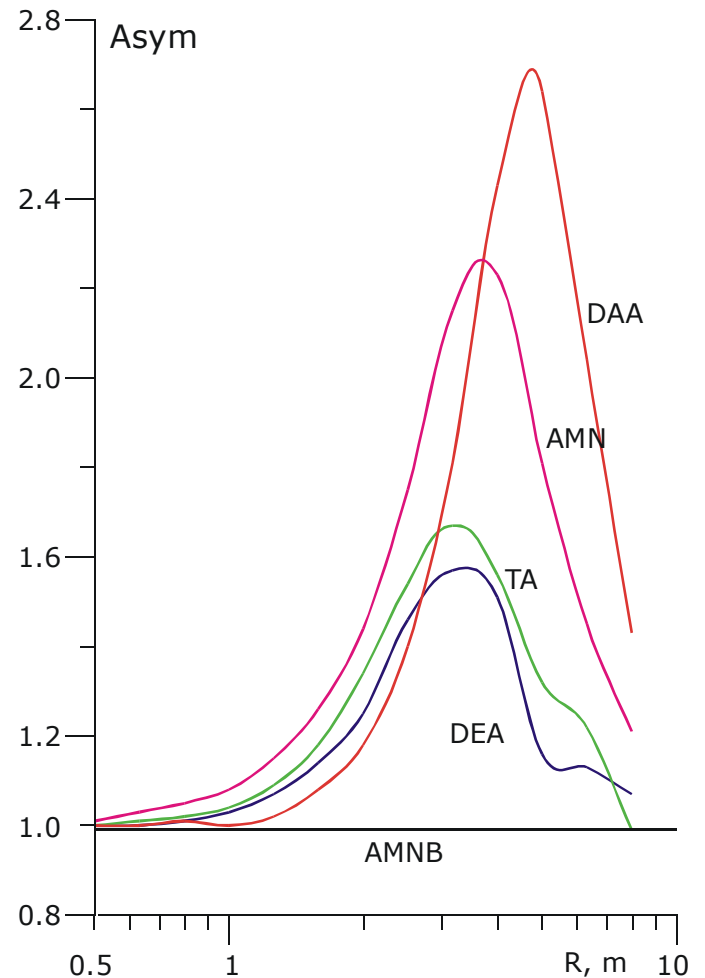

Fig.7. The asymmetry diagrams for different arrays.

5

influence exceeding pseudo-anisotropy influence. For dipping interface with isotropic basement (pseudo-anisotropy case, curve 2 - TAIC, fig.6) the amplitude of the second harmonic for T array at great spacings decreases and becomes 10 times less then the first one.

The graphs of asymmetry factor (Bolshakov et al, 1997) on fig.7 are similar to the graphs of the first harmonic of ARS spectrum (fig.4). They are also similar in physical sense - reflecting only inhomogeneities influence (for arrays on the earth surface). Schlumberger array (5) differs greatly from all, when its rotation is carried out around of array center, its asymmetry factor is always equal to 1 and the array can not diagnoses an inhomogeneity at all. From the others arrays the least sensitivity to inhomogeneity DEA (1) and TA (2) have. The collinear arrays AMN (4) and DAA (3) have greater sensitivity to inhomogeneity then DEA and TA.
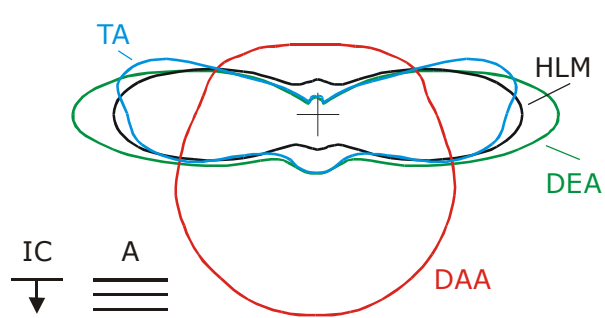

Fig.8. Azimuthal diagrams for 4 arrays for model 4 (fig.1) on 5 m spacing.

On fig.8 the ARS diagrams for different arrays at 5 m spacing for model from fig.1, 4 are shown. The interface dip (IC) in fig.8 is directed downwards, and the strike of an anisotropic formation (A) - is horizontal. The diagrams for horizontally layered model (HLM - DEA array), dipole equatorial and T arrays are similar, and appreciably differ from DAA on sensitivity to anisotropy. The dipole axial array reacts basically on a dipping interface, instead of anisotropy by virtue of its smaller depth of investigation and lowered sensitivity to anisotropy at high sensitivity to an inhomogeneity. This example once again demonstrates problems of anisotropy estimation at the presence of inhomogeneities when collinear arrays are used.

Model with anisotropy strike orientation in parallel to the inclined boundary dip

On fig.9 ARS diagrams (for 3.1 m spacing), similar to fig.8 are given, but for model 3 from fig.1, when the anisotropy strike (A) is parallel to the inclined boundary dip (IC). The diagram for T - array is similar to the case of horizontally - layered medium (HLM) and is extended in the direction of anisotropy strike (A), though the form of the diagram is deformed by the dipping interface influence. The diagram for dipole azimuthal array is extended not on anisotropy strike, but on the dipping interface strike (IC) and appreciably is displaced from the rotation center (diagram center is marked by a cross) in the dip direction, i.e. reflects mainly the dipping interface influence, instead of anisotropy.
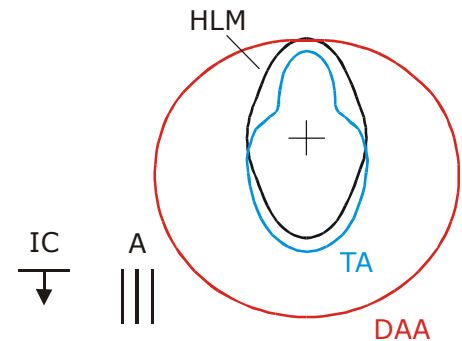

Fig.9. Azimuthal diagrams for T and DA arrays for model 3 (fig.1) at spacing 3.1 m.

The problem of anisotropy estimation at the presence of inhomogeneities is reflected also on fig.10, where the graphs of the ratio of the sums odd to the sum of even harmonics of a spectrum are displayed. This parameter (Bolshakov et al., 1997) reflects the balance of inhomogeneity and anisotropy influences. When the parameter's value is more than 1, the inhomogeneity influence prevails (filled area on fig.10, marked with letter U - unfavorable), and when it is less than 1 - anisotropy influence prevails (an area marked with letter F - favorable). For nonlinear T array at spacings more than 3 m the anisotropy influence prevails, and for collinear DA array - inhomogeneity influence prevails at all spacings, though anisotropy coefficient of the basement is rather high (λ=2), and the inclined contact dip is only 5°. For comparison on fig.11 the similar graphs for isotropic model are shown. In this case on both (T and DA) arrays the only inhomogeneity influence is visible.
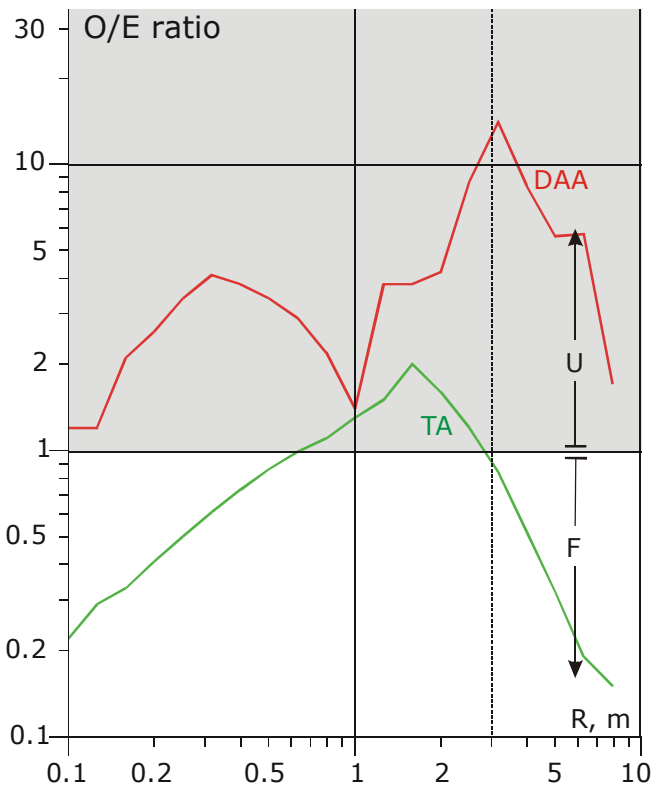
Fig.10. The graphs of the sum of odd to even spectrum's harmonics ratio for T and DA arrays in case of dipping interface with anisotropy. F – favorable O/E ratio.
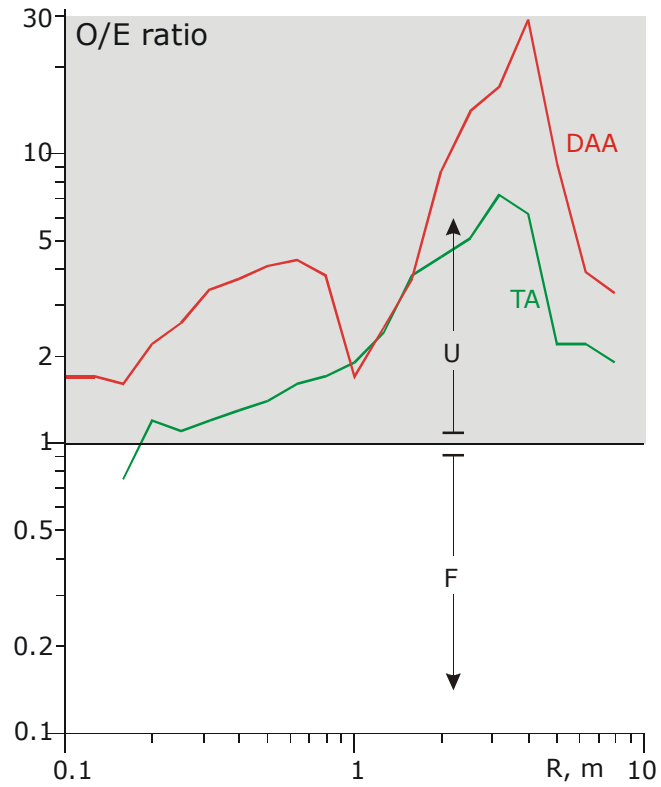
Fig.11. The graphs of the sum of odd to even spectrum's harmonics ratio for T and DA arrays in case of dipping interface without anisotropy. F – favorable O/E ratio.

Model with anisotropy strike orientation at 45° to the dipping interface strike

On fig.12 the ARS diagrams (for 6.3 m spacing), for model, when the anisotropy strike (A) at 45° to the dipping interface strike (IC) are displayed. The diagrams for T- and dipole equatorial (DE) arrays - are similar and are extended in anisotropy strike direction, though the form of the diagrams is distorted a little by the dipping interface influence. The diagram for Schlumberger array (at the given array rotation around of its center) has no visible distortions and is extended along anisotropy strike; the diagram for AMN array is appreciably deformed in comparison with Schlumberger array. The diagram for dipole azimuthal array is mostly deformed and displaced from the rotation center (center of the diagram) in the direction of inclined interface dip; the determination on it the dipping interface strike or anisotropy strike is difficult.

On fig.13 the similar diagrams, but for model $\rho_2 > \rho_1$ at 10 m spacing are displayed. Ellipticity of the diagram for DE array in this case is appreciable less, both for horizontally - layered model (1) and for dipping interface with the anisotropic basement (3). The difference of the diagrams for layered medium and dipping interface (1 and 3) is more, than for model on fig.12. The estimation of dipping
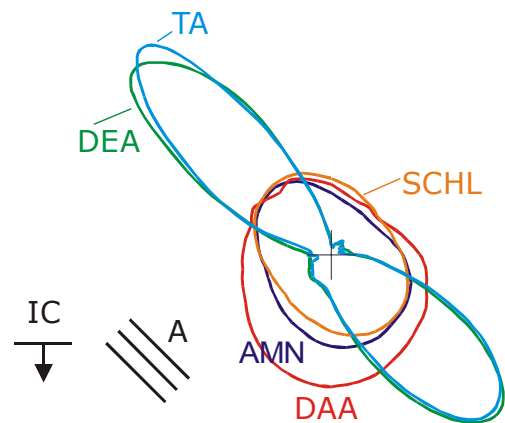

Fig.12. The ARS diagrams for different arrays for anisotropy orientation at 45° at 6.3 m spacing (for model $\rho_2 < \rho_1$).

7

interface or anisotropy strike on DAA diagram is difficult as earlier. But if the diagrams for model $\rho_2<\rho_1$ were extended to inclined boundary dip, these for model $\rho_2>\rho_1$ are extended to the rise direction (fig.13).

On fig. 15 the graphs of the ratio of the sum of odd and even harmonics for two cases $\rho_2<\rho_1$ and $\rho_2>\rho_1$ together with the graphs of apparent anisotropy coefficients (5, 6) are displayed. For collinear array (DAA) on spacings more than 3 m the value of O/E parameter shows prevailing inhomogeneity influence (curves 2, 3), and for nonlinear arrays (TA, DEA) the anisotropy influence (curves 4, 1) prevails. It means, that only nonlinear arrays can estimate an anisotropy among an inhomogeneity influence above such models.

On fig.14 the azimuthal diagrams for isotropic model $\rho_2<\rho_1$ on 6.3 m spacing are submitted. The diagrams ellipticity is not so clear expressed, but the apparent anisotropy coefficient achieves 1.1 for Schlumberger and DAA arrays and 1.02 for T array. This is the pseudo-anisotropy case, when the diagrams' deformation is caused by not anisotropy, but inhomogeneity. The larger axis of the diagrams is guided along the dip of inclined contact (IC). To distinguish this case from anisotropic model it is necessary to calculate the ratio an odd and even components of a spectrum.

Fig.13. The ARS diagrams for DE and DA arrays for anisotropy orientation at 45° at 10 m spacing for model $\rho_2>\rho_1$.

Fig.14. View of azimuthal diagrams for 3 arrays for model 2 (fig.1) on spacing of 6.3 m.
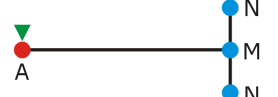
Fig.15. The graphs of odd and even harmonics of spectrum ratio for several arrays and two models $\rho_2<\rho_1$ (R1) and $\rho_2>\rho_1$ (R2). F – favorable O/E ratio.

Such graphs for TA and DAA arrays were given on fig.11 and confidently allowed to determine prevailing influence of an inhomogeneity. For Schlumberger array this parameter was not considered, as for symmetric array rotation there is no sense in it.

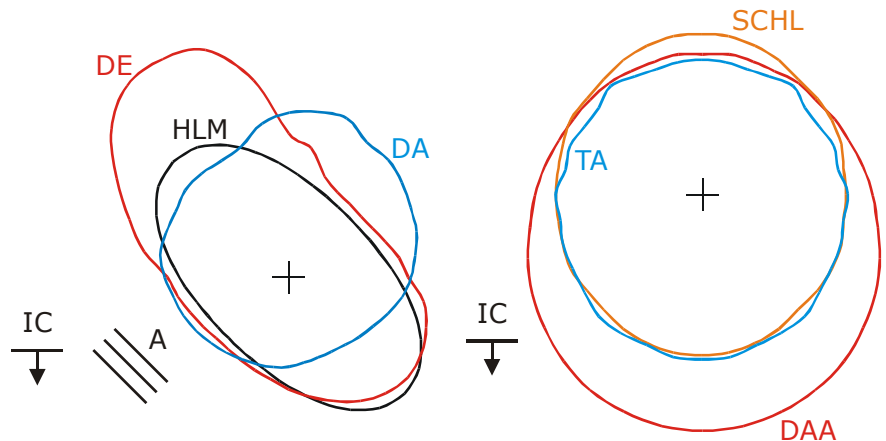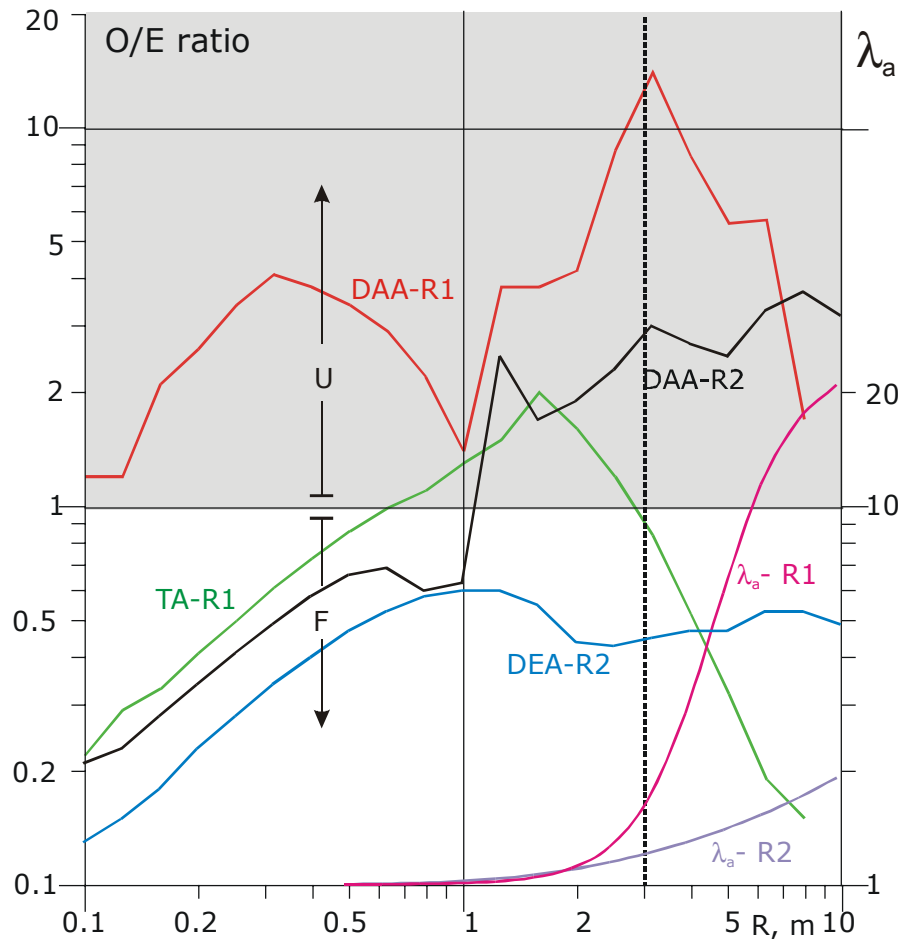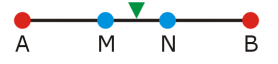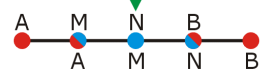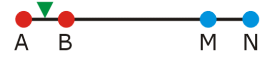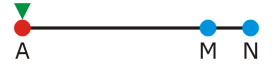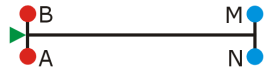Main properties of different arrays considered here have been summarized in table 1.

Table 1. Arrays' properties for comparative anisotropy and inhomogeneity influence.

Type of array and its rotation center ▼	Influence of inhomogeneity (**I**) and that of anisotropy (**A**)	Sensitivity to inhomo-geneities	Sensitivity to aniso-tropy λ^n, n =(1 - 5)	Break in anisotropy paradox at sounding Yes ●/ No ○	Speed and effectiveness of azimuthal sounding technology
Schlumberger or Wenner	No difference between (**I**) and (**A**).	○○○	●○○○○	●	●●●●●
Offset - Wenner (OW)	Clear difference (**I**) and (**A**). Great step in their discrimination	●●○	●○○○○	●	●●●●●
Dipole axial	(**I**) >> (**A**)	●●●	●○○○○	●	●●●●○
Pole-dipole	Similar to OW	●●○	●○○○○	●	●●●●○
Dipole – equatorial	(**A**) > (**I**)	●○○	●●●●●	○	●●●○○
T – array	(**A**) > (**I**)	●○○	●●●●●	○	●●●○○

Non-linear arrays now have not fast and effective field technology of azimuthal sounding, compared with Offset-Wenner field technology (Watson and Barker, 1999, Watson, 1999). All other properties are better for non-linear arrays. The most promising for fast field azimuthal sounding is the Arrow – type array (Bolshakov et al., 1998b).

Conclusions

1. The dipole axial array is the most sensitive to dipping interface. Pole-dipole and dipole equatorial arrays follow it in sensitivity decreasing. On sensitivity to an anisotropy all of array are divided into two groups: collinear arrays (Schlumberger, pole-pole, pole-dipole, dipole axial array) with the axes ratio of ARS diagrams equal λ, and non-collinear (non-linear) arrays with sensitivity up to λ^5 (DE array, T-array, etc.).

2. In models with a weak inhomogeneity influence, the linear approach to decomposition of inhomogeneity and anisotropy influence at a level of spectra can be applied. In the case of current and

measuring electrodes' arrangement on the earth surface, the inhomogeneity is displayed in the first harmonic of a spectrum, and anisotropy - in the second harmonic. The inhomogeneity also influences on the second harmonic. The absence of the first harmonic (and following odd ones) testifies to absence of inhomogeneities' influence. As the second harmonic of a spectrum can be caused both anisotropy and inhomogeneity, it is necessary to consider the ratio of the sum of odd to the sum of even harmonics. When this ratio is more than one, the inhomogeneity influence prevails, and when it is less than one - the anisotropy influence prevails. For reception of the azimuthal diagrams, correctly reflecting the inhomogeneity and anisotropy influence, an asymmetrical array rotation on 360° is absolutely necessary. At joint influence of the basement anisotropy (λ=2) and dipping interface (dip is 5°) only non-collinear arrays reflect the anisotropy influence stronger, than the inhomogeneity influence. For collinear arrays above such models the estimation of anisotropy parameters is difficult because of stronger inhomogeneity influence.

3. At identical spacings and arrays the anisotropy influence has the stronger effect in model with the conducting basement $\rho_2 < \rho_1$, then in case of resistive basement $\rho_2 > \rho_1$.

Acknowledgments

References

1. Bolshakov D.K., Modin I.N., Pervago E.V., Shevnin V.A. Separation of anisotropy and inhomogeneity influence by the spectral analysis of azimuthal resistivity diagrams. *Proceedings of 3rd EEGS-ES Meeting*. Aarhus, Denmark, 8-11 Sept 1997. P.147-150.
2. Bolshakov D.K., Modin I.N., Pervago E.V., Shevnin V.A. Modeling and interpretation of azimuthal resistivity sounding over two-layered model with arbitrary - oriented anisotropy in each layer. *EAGE 60th Conference*, Leipzig - 1998. P110.
3. Bolshakov D.K., Modin I.N., Pervago E.V., Shevnin V.A. New step in anisotropy studies: arrow-type array. *Proceedings of 4th EEGS-ES Meeting*. Barselona, Spain, September 1998. P. 857-860.
4. Electrical prospecting by resistivity method. *MSU edition*, Moscow, 1994, 160 pp. (In Russian).
5. A.Mousatov, E.Pervago, V.Shevnin. New approach to resistivity anisotropic measurements. *Proceedings of SEG 70th Annual Meeting*. Calgary, Alberta, Canada, August 6-11, 2000, 4 pp. NSG-P1.5.
6. Semenov A.S. Rock anisotropy and electrical fields peculiarities in anisotropic media. *Vestnik of Leningrad university*, ser. Geology and geography. 1975. N 24. P.40-47. (In Russian)
7. Watson K.A. and Barker R.D. Differentiating anisotropy and lateral effects using azimuthal resistivity offset Wenner soundings. *Geophysics*, 1999, Vol.64, N 3, p.739-745.
8. Watson, K.A. 1999. Differentiating anisotropy and lateral effects using azimuthal resistivity offset Wenner soundings. *Unpublished Ph. D. Thesis*, School of Earth Sciences. Faculty of Science. University of Birmingham.